RSC Advances

ROYAL SOCIETY OF CHEMISTRY

www.rsc.org/advances

Journal Name

RSCPublishing

ARTICLE

The Synergistic Mechanism of Phytic Acid Monolayers and Iodide Ions for Inhibition of Copper Corrosion in Acidic Media†

Shu Shen, Cheng-di Zhu, Xiao-yu Guo, Chuan-chuan Li, Ying Wen, Hai-Feng Yang*

Cite this: DOI: 10.1039/x0xx00000x

Received 00th January 2012,
Accepted 00th January 2012

DOI: 10.1039/x0xx00000x

www.rsc.org/

The adsorption behavior of phytic acid (PA) self-assembled monolayers (SAMs) at the copper surface, and its corrosion inhibition mechanism in 0.5 M H_2SO_4 solution, was studied by using electrochemical impedance spectroscopy (EIS), potentiodynamic polarization and surface-enhanced Raman scattering spectroscopy (SERS). Raman studies showed that PA SAMs on the copper surface formed via P-O and the cyclohexyl ring. The adsorption of PA SAMs on copper surface followed Langmuir isotherm and revealed a chemical adsorption on the copper surface. The presence of I^- ions with PA SAMs at the copper surface showed a synergistic effect and increased the inhibition efficiency.

1. Introduction

Copper and its alloys have been used in various ways of industrial and microelectronic applications due to its good thermal, electrical conductivity, mechanical workability, and relatively noble properties [1-5]. However, copper and its alloys easily suffer from severe corrosion, especially in the aggressive environment. Industrial acids are extensively employed in many industrial processes, including acid pickling and acid descaling as well as in oil well acidification, which cause the damage of copper. For example, sulphuric acid solution is one of the most commonly used industrial acids [6].

Organic inhibitors containing nitrogen, oxygen or sulphur atoms are usually used to mitigate the electrochemical corrosion attack against metal materials [7-11]. But the usage of these organic inhibitors not only results in the economic cost but also causes the release of toxic substances into the environment.

From a green chemical view, we once introduced a kind of green molecules, phytic acid (PA) and its salts, which could be used as the corrosion inhibitors in salt solution [12]. PA contains six phosphoric acid groups which can interact with the metal ions (see Scheme S1 in supplementary materials). The most attractive advantage of PA is its availability as a naturally polyphosphorylated carbohydrate, widely occurring in beans, brownrice, corn, sesame seeds, and wheat bran. The use of PA as the cleansing agent, water treatment agent, food additive and cosmetic additive proves that it is non-toxic to human and "green" to the environment [13-19].

Meanwhile, synergistic effect, which can highly improve the performance of the corrosion inhibitor compared with the inhibitor alone, has been proven to be an effective mean to enhance the inhibitive ability and diversify the application of inhibitor in acidic media [20-22]. The synergistic effect of halides has been reported to be in the order: $I^- >> Br^- > Cl^-$. The highest synergistic effect of I^- ions is due to the chemisorption onto metal surface with its larger size and ease of polarization [23, 24].

In our previous work involving copper protected by PA in 3% NaCl solution, the inhibition efficiency was below 90% [12]. In this work, we attempted to improve the inhibition effect of PA self-assembled monolayers (SAMs) on the copper in 0.5 M H_2SO_4 solution by the addition of I^- ions. SAMs technique is regarded as an easy method to form dense and ordered monolayers, acting as effective barrier to protect the copper against corrosion [25-27]. The inhibition behavior was undertaken using electrochemical impedance spectroscopy (EIS), electrochemical polarization and surface-enhanced Raman scattering spectroscopy (SERS). SERS is a highly sensitive technique for probing the monolayer adsorption behavior of the molecule on a metal surface [28-30]. Additionally, the adsorption behavior of PA SAMs was investigated by Langmuir adsorption isotherm.

2. Experimental Section

2.1. Materials and chemicals

PA (50 wt%) solution was purchased from the Sigma-Aldrich Corporation. Sulphuric acid, potassium iodide, and ethanol were of analytical grade and purchased from Sinopharm Chemical Reagents Company. Electrochemical experiments were undertaken in 0.5 M H_2SO_4 solution in the absence and presence of different concentrations of PA, KI and mixture solution of 0.1 mM PA and KI, respectively. The KI concentration in the mixture solution was varied in the range of 1-5 mM. All the solutions were prepared with Milli-Q water (18 MΩ cm).

2.2. Apparatus

Raman spectroscopic measurements were obtained on a confocal microprobe Raman system (LabRam II, Dilor, France), with a holographic notch filter and a liquid–nitrogen–cooled CCD detector. A He–Ne laser at 632.8 nm with a power of ca 5 mW was used as the excitation source for the Raman experiment. A 50×long-working-length objective was used to focus the laser spot onto the electrode surface. The slit and pinhole were set at 100 and 1000 μm, respectively. Each spectrum was measured 3 times and the acquisition time was 15 s. Calibration was done referring to the 519 cm^{-1} line of silicon line.

The electrochemical measurements were carried out by a CHI750c electrochemistry workstation (CH Instruments, Inc.).

2.3. Pretreatment for electrodes

The copper electrode was made from the polycrystalline copper rod (99.999%, Sigma-Aldrich) and the geometric area of surface was ca. 0.0314 cm^2 (embedded in a Teflon sheath). Before all the experiments, the copper electrode was sequentially polished with emery paper and 0.3 μm alumina/water slurries until a shiny, mirror-like surface was obtained, and then was ultrasonically washed with Milli-Q water and pure ethanol to remove any existed alumina particles. For SERS detection, to obtain the necessary roughness of the copper surface, an oxidation reduction cycle treatment (ORC) was performed in a conventional three-electrode cell [31]. The bare copper specimen or the PA SAMs modified copper specimen was used as the working electrode. A platinum electrode was used as the counter electrode and the reference electrode was a saturated calomel electrode (SCE). All potentials cited in this paper were converted to SCE.

2.4. Self-assembled monolayers

To form the monolayers, the polished copper electrode was underwent ORC in 2 M H_2SO_4 by switching between -550 and +450 vs mV/SCE to achieve a fresh and oxide-free surface, then rinsed with Milli-Q water and absolute ethanol as soon as possible. After that the copper electrode were immersed immediately into the deoxygenated different concentrations of PA, KI solution and mixture solution of PA and KI for different time at room temperature. Finally, the coated electrode was taken out of the solutions and rinsed carefully with ethanol and Milli-Q water, then subsequently dried by flowing nitrogen gas prior to the further investigations.

2.5. Electrochemical measurements

The electrochemical studies were carried out in a three-electrode cell assembly. EIS measurements were performed at the open circuit potentials with the AC voltage amplitude of 5 mV in the frequency range from100 kHz to 0.01 Hz. The polarization curves were obtained from +200 to -300 vs mV / SCE with a scan rate of 10 mV s^{-1}.

3. Results and discussion

3.1. Inhibition by PA SAMs

3.1.1. Electrochemical impedance measurement

EIS technique, a nondestructive, sensitive, and informative method, has been extensively used for the evaluation of coatings on metal surface for corrosion inhibition, especially for analyzing the surface with SAMs. Nyquist plots for copper in 0.5 M H_2SO_4 solution (with and without PA SAMs) for the same assembled time (4h) are presented in Figure 1 and the corresponding impedance parameters are given in Table 1. Nyquist plots and data for copper electrodes without and with PA SAMs formed at different assembled time in 0.5 M H_2SO_4 solution are given out in supplementary materials.

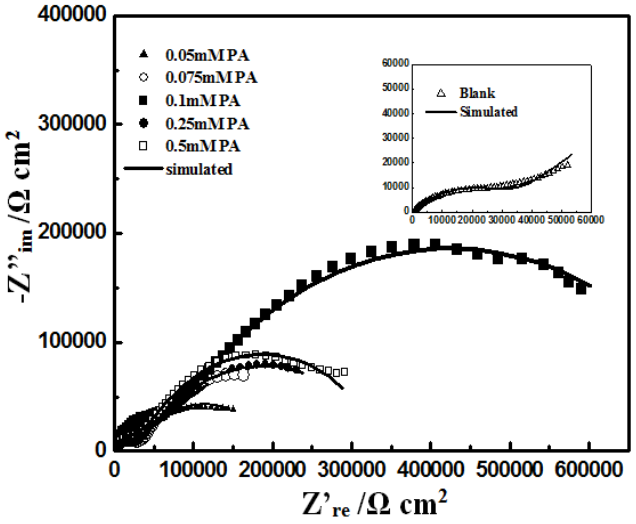

Figure 1. Nyquist plots of copper electrodes in 0.5 M H_2SO_4 solution with PA films formed from different concentrations of PA solutions for 4 h. The inset is the Nyquist plots of blank copper.

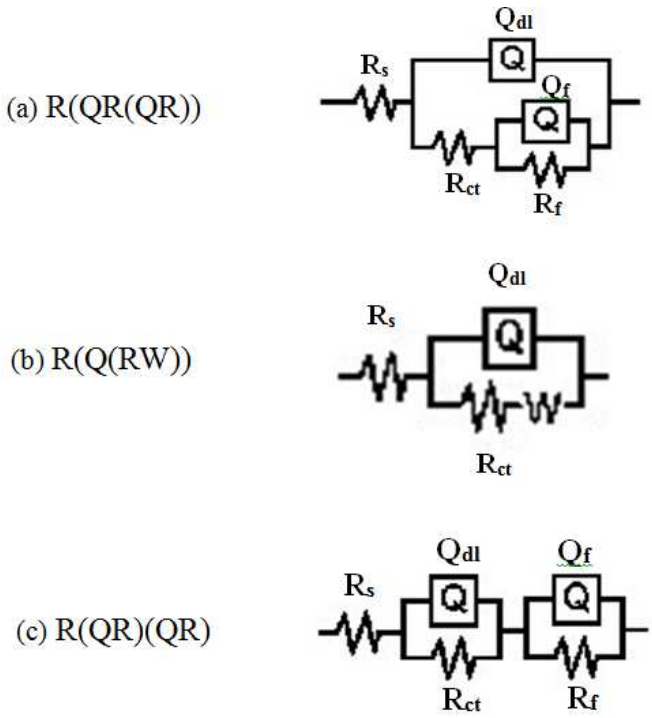

Scheme 1. Electrical equivalent circuit models for impedance data: (a) in the presence of PA SAMs; (b) bare copper and copper with KI adsorption from different concentrations of KI solutions; (c) in the presence of PA film formed in 0.1 mM PA solution in combination of different KI solutions.

The equivalent circuits analyzed by ZsimpWin software are presented in Scheme 1. R(Q(RW)) and R(QR(QR)) are suitable for the Nyquist plots of the coppers without and with PA SAMs

respectively. R_s is the resistance of the solution, R_{ct} is the charge-transfer resistance in high frequency, R_f is the film resistance related

Table 1. EIS parameters of copper electrodes in 0.5 M H_2SO_4 solution with PA SAMs formed from different concentrations of PA solutions for 4 h.

Concentration (mM)	R_s (Ω cm^2)	Q_{dl}(μY^a)	n	R_{ct} (kΩ cm^2)	Q_f(μY^a)	n	R_f (kΩ cm^2)	W ($\mu\Omega$ cm^2)	η(%)
Blank	489.3	1.101	0.80	112.28				0.1142	
0.05	277.8	1.713	0.61	27.80	0.1155	0.67	247.4		59.2
0.075	374.5	0.4164	0.80	28.20	18.41	0.80	374.2		72.1
0.1	300	0.2017	0.77	72.41	2.692	0.58	652.0		84.5
0.25	410.5	0.2068	0.83	22.47	0.1339	0.55	389.51		72.7
0.5	594.9	0.520	0.80	39.92	5.047	0.80	379.0		73.2

[a]The dimensions are S; s^n/cm^2; if n = 1, they are F cm^{-2}

to the adsorption of inhibitor molecules and all other accumulated species on metal/solution interface in region of low frequency [32-34], Q_{dl} and Q_f stand for the constant phase elements (CPE), representing double-layer capacitance and film capacity, and W is Warburg impedance. The impedance function of the CPE is described by the following equation:

$$Z_{CPE} = Y_0^{-1}(j\omega)^{-n} \quad (1)$$

where Y_0 is the modulus, j is the imaginary root, ω is the angular frequency and n is the phase. Depending on the value of the exponent n, Q may be a resistance, R (n = 0); a capacitance, C (n = 1); Warburg impedance, W (n = 0.5), or an inductance, L (n = -1). The value range of a real electrode of n is often between 0 and 1, showing the phase shift that can be explained as the degree of surface inhomogeneity [35]. In the present fitting, all the χ^2 values of the blank and modified electrodes are around 1×10^{-3} and the acceptable errors of EIS elements in fitting mode are below 10%.

The Nyquist plot of bare copper (the inset picture) displays a straight line at low frequencies (Warburg impedance) and a small semicircle (R_{ct}) in region of high frequency. The Warburg impedance in low frequency region is due to the diffusion process of soluble copper species from the electrode surface to the bulk solution [36].

However, the Nyquist plots of PA SAMs covered copper electrodes have two semicircles, which are different from that of bare copper. The small semicircle is related to the R_{ct} in region of high frequency. The appearance of R_f in region of low frequency means that the PA SAMs have formed on the copper surface, which can obviously increase the resistance of the copper surface and protect the copper from corrosion. In region of low frequency, compared with the blank copper, the Warburg impedance disappears in the PA SAMs coated copper surface, indicating the formation of PA SAMs on copper electrode can significantly inhibits the diffusion process of soluble copper species from the electrode surface to the solution. The semicircles in Nyquist plots show that the rise in different concentrations results in the increase in diameter and it reaches maximum under the concentration of 0.1 mM.

The inhibition efficiency (η) obtained from Table 1 can be calculated according to the following equation [37]:

$$\eta(\%) = \frac{R_p - R_p^0}{R_p} \times 100 \quad (2)$$

where R_p^0 is the polarization resistance of the naked copper, and R_p is the polarization resistance of the PA SAMs-covered copper electrode. The polarization resistance is the sum of R_{ct} and R_f. The calculated η as an optimum value is 84.5% under the concentration of 0.1 mM and assembled time about 4 h in 0.5 M H_2SO_4 solution (see supplementary material).

3.1.2. Potentiodynamic polarization studies

The electrochemical polarization method can provide the corrosion rate from linear polarization and determine the efficiency of the corrosion inhibitor. Figure 2 shows polarization curves recorded in 0.5 M H_2SO_4 solution in the absence and presence of PA SAMs on the copper surface formed at different immersion time in 0.1 mM PA solution. The corresponding electrochemical parameters such as the corrosion potential (E_{corr}) and corrosion current densities (I_{corr}) along with the inhibition efficiency (η) are listed in Table 2. Both the anodic and cathodic Tafel regions are used to determine the I_{corr} and E_{corr} [38]. The polarization curves and corresponding parameters the copper surfaces in the absence and presence of PA SAMs formed at different concentrations of PA solutions, recorded in 0.5 M H_2SO_4 solution, are displayed as supplementary material.

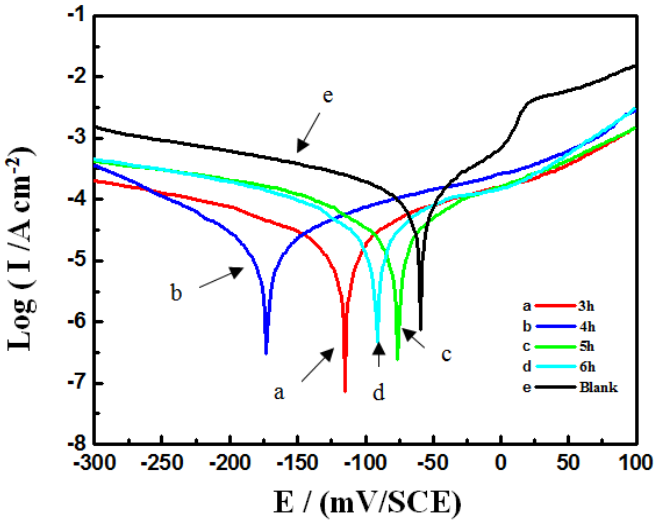

Figure 2. Potentiodynamic polarization curves in 0.5 M H_2SO_4 solution for blank copper electrode and the presence of PA SAMs formed in 0.1mM PA solution for different time.

Table 2. Potentiodynamic polarization parameters for copper in 0.5 M H_2SO_4 solution for blank copper electrode and the presence of PA SAMs formed in 0.1mM PA solution for different time.

time(h)	-E_{corr} (mV)	I_{corr} (μA cm^{-2})	η (%)
Blank	59	166.8	
3	115	34.3	79.5
4	173	27.9	83.3
5	76	54.1	67.6
6	91	70.1	58.0

It can be seen from Figure 2 that, both anodic and cathodic current densities of the copper electrodes with PA SAMs decrease obviously at the same potential compared with the bare electrode, demonstrating that the formation of PA SAMs inhibit anodic and cathodic reaction processes simultaneously. Nevertheless, the cathodic reaction is inhibited to a larger extent compared with the anodic reaction. An inhibitor can be classified as an anodic or cathodic type inhibitor based on the difference between corrosion potential (E_{corr}) values of copper electrodes with and without film

which is larger than 85 mV or not [39]. Herein, most of the displacement in E_{corr} value is below 85 mV. Therefore, PA might act as a mixed type inhibitor with predominantly cathodic inhibitor. The negative shift of E_{corr} could be explained by the fact that the inhibitor has a stronger influence on the oxygen reduction (cathodic reaction) than on the copper dissolution reaction (anodic reaction). Therefore, PA SAMs suppress the transfer of O_2 to the cathodic sites of the copper surface, decreasing the rate of oxygen reduction. The corresponding inhibition efficiency is calculated using the following equation [40]:

$$\eta(\%)=\frac{I_{corr(a)}-I_{corr(b)}}{I_{corr(a)}}\times 100 \quad (3)$$

where $I_{corr(a)}$ and $I_{corr(b)}$ are the corrosion current densities in the absence and presence of PA SAMs on the copper surface, respectively.

After immersed in 0.5 M H_2SO_4 solution, all the corrosion current density of the coated copper electrodes are lower than that of the bare copper electrode. The inhibition efficiency (83.3%) of the copper electrode with PA SAMs formed for 4 h assembled time is higher than the others. The SAMs can only be formed under the proper assembled time and the concentration of inhibitor. In this work, the optimized assembled time is 4 h.

3.1.3. Raman study

The presence of PA SAMs can be detected by SERS spectroscopy in Figure 3a and their assignments for PA SAMs observed vibrations are also summarized in Table 3, based on the vibrational calculation of PA using the B3LYP/LANL2DZ method in Gaussian 03 programs [15]. Because of its good chemical activity and SERS-active substrate treatment under the ORC condition, the copper oxide layers are inevitably formed. The bands around 532 and 594 cm^{-1} are due to the oxide species of copper [13].

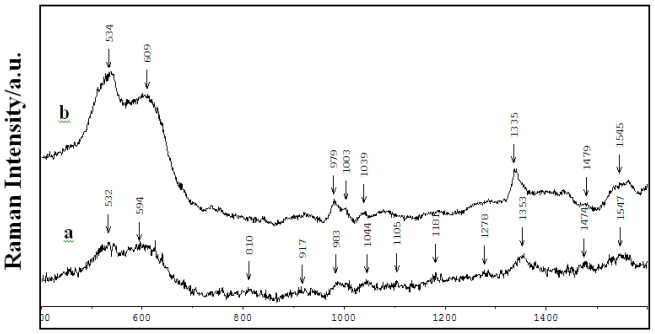

Figure 3. SERS spectrum of copper electrode with (a) PA film formed in 0.1mM PA solution for 4 h; (b) PA film formed in 0.1 mM PA solution in combination with 5 mM KI.

Some bands at 810, 983, 1044, 1278 and 1353 cm^{-1} are ascribed to P^{43}-O^{42}-C^{41} rock stretching, P^{43}-O^{42}-C^{41} stretching, P^{35}-O^{36} stretching, P^{43}-O^{42}-C^{41} asymmetrical stretching and P^{27}-O^{28} stretching, respectively. The peaks at 917 and 1105 cm^{-1} are all relative to the vibrations of the cyclohexyl ring. It has been generally accepted that, the SERS mechanism [41, 42] and the surface selection rule [43, 44], the vibrational modes of groups that attach to or are very close to the surface should be more enhanced in the SERS spectrum and the vibrational modes with parallel polarizability components with respect to the surface will not be enhanced. Therefore, the SERS peaks regarding P-O are enhanced by the surface, meaning the P-O groups attach onto the surface and their vibration modes of stretching are with respect to the surface. The occurrence of carbon skeleton stretching beside P^{43}, P^{35} and P^{27} and two peaks at 917 and 1105 cm^{-1} from the vibrations regarding the cyclohexyl ring hints that the cyclohexyl ring approaches the copper surface with a tilted way. The above SERS observations suggested that the PA molecule adsorbed at the surface via the P^{27}, P^{35}, and P^{43} atoms and the cyclohexyl ring being closer to the surface. As a result, PA SAMs are able to show the relatively high corrosion efficiency over 80%.

Table 3. Assignments for SERS Spectrum of PA SAMs and PA SAMs with I^- ions.

PA (cm^{-1})	PA + KI (cm^{-1})	PA calcd (cm^{-1})	Approximate[a] assignment
810w		808	P^{43}-O^{42}-C^{41} rock. C^{31}-H, C^{8}-H. ip.bend.
917w		924	cycl. ring. breath.
983w	979s	989	C^{8}-C^{41}-C^{33} as.
	1003w		P^{43}-O^{42}-C^{41} str.
1044m	1039w	1025	P^{43}-O^{42}-C^{41} as., C^{41}-C^{8}-C^{9} ip bend.
1105w		1132	cycl. ring.bend.
1181w		1204	C^{25}-H, C^{17}-H, C^{9}-H, C^{8}-H op.bend.
1278w		1279	P^{35}-O^{36} str. C^{33}-H, C^{25}-H, C^{17}-H ip.bend
1353s	1335s	1318	P^{27}-O^{28} str.
1474m	1479w	1482	C^{41}-H, C^{8}-H op.bend
1547s	1545w	1529	C^{25}-H, C^{17}-H, C^{9}-H op.bend

[a]Abbreviations used: s, strong; m, medium; w, weak; br, broad; bend, bending; str., stretching; ip, in-plane; op,out plane;as, asymmetric;

Figure 3b is the SERS spectrum of the copper surface in the presence of PA film together with 5 mM KI. Compared with the SERS spectrum of the copper surface with PA film only, the two bands at 979 cm^{-1} and 1335cm^{-1} are enhanced and blue shifted. Some bands, such as 810, 917, 1105, and 1278 cm^{-1} disappear. All these phenomena result from the effect of I^- on the PA film. The PA molecules adsorbed at the copper only adopt P^{43} and P^{27} atoms.

3.1.4. Adsorption isotherm

The establishment of adsorption isotherm can provide valuable information on the nature and strength of adsorption of organic compounds on metal surface. Therefore, the investigation of relationship between the adsorption and corrosion inhibition is important [45]. Assuming a direct relationship between inhibition efficiency (η%) and surface coverage (θ) [η% = 100 × θ] for different inhibitor concentrations, data obtained from EIS measurements [46, 47] are used to determine the adsorption characteristics of PA SAMs on copper surface in 0.5 M H_2SO_4 solution. To clarify the nature of adsorption, theoretical fitting to different isotherms is undertaken and the correlation coefficients (r^2) are used to determine the best fit, which is obtained with the Langmuir isotherm (r^2 = 0.999). The Langmuir isotherm can be described as the following equation [48, 49]:

$$\frac{C}{\theta}=\frac{1}{K_{ads}}+C \quad (4)$$

where C is the inhibitor concentration, θ is the degree of surface coverage and K_{ads} is the equilibrium constant related to the free energy of adsorption ΔG^0_{ads} by the equation:

$$\Delta G^0_{ads}=-RT\ln(55.5K_{ads}) \quad (5)$$

where R is the universal gas constant and T is the absolute temperature. The value of 55.5 is the concentration of water in solution expressed in mole.

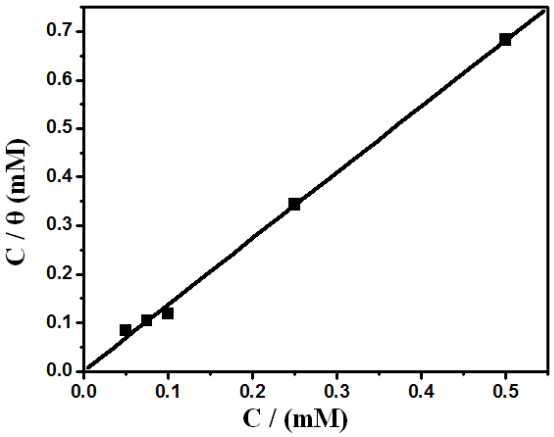

Figure 4. Langmuir adsorption isotherm for PA SAMs on the copper in 0.5 M H_2SO_4 solution at 25°C.

The plot of C/θ vs C is shown in Figure 4 to be linear. The adsorption equilibrium constant (K_{ads}) obtained is 8.33×10^5 M^{-1}, indicating that the PA SAMs possesses strong adsorption ability onto the copper surface [50]. The value of ΔG^0_{ads} up to -38.02 kJ mol^{-1} also indicates the strong interaction between inhibitor molecules and the copper surface, spontaneity of the adsorption process and stability of the adsorbed layer on the copper surface. It is well known that the values of ΔG^0_{ads} in the order of -20 kJ mol^{-1} or less negative are associated with an electrostatic interaction between the charged inhibitor molecules and the charged metal surface (physical adsorption) [51]; those of -40 kJ mol^{-1} or more negative involves charge sharing or transferring from the inhibitor molecules to the metal surface to form a coordinate covalent bond (chemical adsorption) [52, 53]. The calculated value of ΔG^0_{ads} close to -40 kJ mol^{-1} suggests that the adsorption mechanism of PA SAMs on the copper surface is a chemical adsorption. Chemical adsorption might be due to the interaction of unshared electron pairs or p-electrons of the adsorbate with the metal in order to form a coordinate type of bond.

3.2. Synergistic effect of iodide ions

3.2.1. Effect of iodide ions

Halide ions are known to enhance the adsorption of some organic cationic inhibitors on metal surface, thereby improving their inhibition efficiency considerably. This phenomenon, ascribed to as synergistic effect, is often most pronounced with I^- ions.

Table 4. Potentiodynamic polarization parameters for copper in 0.5 M H_2SO_4 solutions containing different concentrations of KI and in combination of 0.1 mM PA SAMs formed in 0.1 mM PA solution.

concentration (mM)	$-E_{corr}$ (mV)	I_{corr} (μA cm^{-2})	η (%)
Blank	59	166.8	
1	55	83.9	49.7
2.5	54	81.8	50.9
5	35	75.8	54.6
1+0.1 PA	78	55.3	66.9
2.5+0.1 PA	136	23.4	86.0
5+0.1 PA	151	16.8	89.9

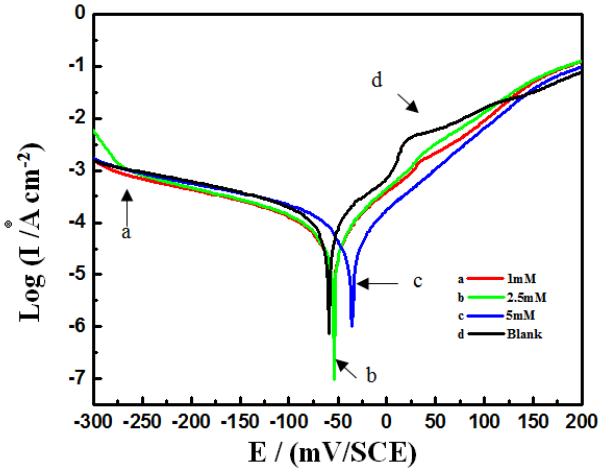

Figure 5. Potentiodynamic polarization curves for copper electrode with and without KI adsorption formed in different concentrations of KI solutions for 2 h in 0.5 mM H_2SO_4.

Figures 5 and 6 are the electrochemical experiments undertaken to assess the effect of addition of I^- ions on the corrosion inhibition performance in 0.5 M H_2SO_4 for 2h. The corresponding parameters are listed in Tables 4 and 5. The impedance data are analyzed using the equivalent circuit shown in Scheme 1(b). The values of inhibition efficiencies obtained are used Equations (2) and (3). The potentiodynamic polarization curves in Figure 5 indicate that the presence of I^- ions slightly shifts the corrosion potential to more positive direction and reduces both the rate of anodic and cathodic reactions. The bigger semicircle of 5 mM KI in Figure 6 shows that higher concentration of KI has better corrosion inhibition.

Table 5. EIS data for copper electrode with and without KI adsorption formed in different concentrations of KI solutions for 2 h in 0.5 mM H_2SO_4.

concentration (mM)	R_f(Ω cm^2)	Q_f (μY^a)	n	R_{ct}(kΩ cm^2)	W (kΩ cm^2)	η (%)
1	181.4	4.44	0.49	200.7	0.3916	44.1
2.5	326.6	4.72	0.80	227.23	0.3416	50.6
5	316.4	0.14	0.80	237.52	0.265	52.7

[a]The dimensions are S; s^n/cm^2; if n = 1, they are F cm^{-2}

3.2.2. Synergistic effect and inhibition mechanism

In 0.5 M H_2SO_4 solution, the impedance behavior of copper with the mixed film formed in solutions containing 0.1 mM PA with different concentrations of KI for 4h are shown in Figure 7. The impedance data are analyzed using the equivalent circuit simulation shown in Scheme 1(c) and the corresponding electrochemical parameters are given in Table 6. The results show that both the R_{ct} and R_f increase with the increasing concentration of KI. The inhibition efficiency increased from 86.0% to 89.9% in the presence of 0.1 mM PA on addition of 2.5 mM and 5 mM KI, which are higher than that of the PA SAMs alone.

The effect of I^- ions on the polarization behavior of copper in the presence of different concentrations of KI in combination with 0.1 mM PA are depicted in Figure 8 and Table 4. From Figure 8, it is clearly seen that the combination of PA SAMs and KI reduce remarkably the anodic and cathodic reactions and decrease considerably the corrosion current densities compared to the blank

copper and 0.1 mM PA SAMs alone, leading to higher inhibition efficiency (89.9 %). The results obtained from polarization and EIS techniques follow the same trend and are in close agreement. The enhanced inhibition efficiency noted for PA SAMs on addition of I^- ions is due to the synergistic effect [54].

The existence of synergism phenomenon between PA SAMs and iodide ions was further evaluated by estimating the synergism parameter (S_1) from the inhibition efficiency values from the two techniques employed according to the following equation [55-57]:

$$S_1 = \frac{1 - I_{1+2}}{1 - I'_{1+2}} \quad (6)$$

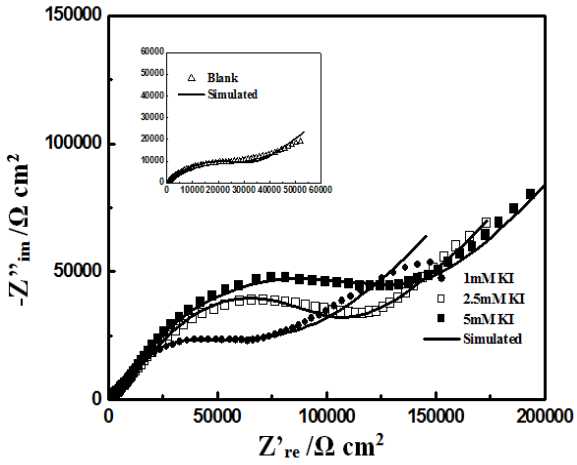

Figure 6. EIS curves for copper electrode with and without KI adsorption formed in different concentrations of KI solutions for 2 h in 0.5 mM H_2SO_4.

Table 6. EIS data for copper in 0.5 M H_2SO_4 solution with the presence of various concentrations of KI + 0.1 mM PA SAMs

concentration (mM)	R_s (Ω cm²)	Q_d (μY[a])	n	R_{ct} (kΩ cm²)	Q_f (μY[a])	n	R_f (kΩ cm²)	η (%)
1+0.1 PA	251.3	6.881	0.52	18.74	1.262	0.79	277.3	62.6
2.5+0.1 PA	557	7.124	0.81	343.7	1.387	0..61	520.0	87.0
5+0.1 PA	128.3	4.544	0.73	105.21	1.113	0.74	947.3	90.0

[a]The dimensions are S; s^n/cm^2; if n = 1, they are F cm^{-2}

where $I_{1+2} = I_1 + I_2$; I_1 is inhibition efficiency of the iodide ions, I_2 is the inhibition efficiency of PA SAMs alone and I'_{1+2} is measured inhibition efficiency for the PA SAMs with the I^- ions. If there is no effect between PA SAMs and I^- ions each other and they are adsorbed at the metal/solution interface independently, then S_1 is equal to 1. Alternatively, synergistic effect manifests when $S_1 > 1$ and antagonistic effect prevails at $S_1 < 1$ [58]. The values of the S_1 for the 2.5 and 5 mM KI with PA SAMs in Table 7 are greater than unity, indicating that there is synergistic effect between PA SAMs and I^- ions in 0.5 M H_2SO_4 solution. However, it is worth mentioning that the case of PA SAMs with 1mM KI may be an exception. The inhibition efficiency in potentiodynamic polarization and EIS methods of 1mM KI are both lower than those of 0.1 mM PA SAMs alone and the synergistic parameter is low than unity. This phenomenon could be ascribed to the antagonistic effect due to the low concentration of KI solution.

In literature [59-61], the authors explained the synergistic effect by initial contact adsorption of iodide ions on the copper surface, followed by a decrease in the positive charge on the metal, which facilitates the adsorption of protonated inhibitors. In another word, the presence of I^- ions on the copper surface could form the interconnecting bridge between the copper surface and the positive charged inhibitor molecules, improving the corrosion inhibition.

It was reported [47, 62] that, the copper surface was positively charged in H_2SO_4 solution. PA molecule can be expected to be protonated in equilibrium with the corresponding neutral form in strong acid solutions.

$$PA + H^+ \leftrightarrow PAH^+ \quad (7)$$

$$Cu \leftrightarrow Cu^+_{ads} + e^- \quad \text{(fast step)} \quad (8)$$

$$Cu^+_{ads} \leftrightarrow Cu^{2+} + e^- \quad \text{(slow)} \quad (9)$$

where Cu^+_{ads} is an adsorbed specie at the copper surface. The reaction equation (9) is controlled by diffusion of soluble Cu^{2+} species from the electrode surface to the bulk solution, which is generally the rate determining step [47].

Due to the electrostatic repulsion, it is difficult for the positively charged inhibitor molecule to approach the positively charged metal surface. In the case of PA SAMs alone, SO_4^{2-} ions should be first adsorbed onto the positively charged copper surface to create an excess negative charge towards the metal to form a protective layer, reducing the corrosion rate of copper [63].

$$Cu^+ + ySO_4^{2-} + xPAH^+ \leftrightarrow \left[Cu - ySO_4^{2-} - xPAH^+\right] \quad (10)$$

where x, and y are the numbers of PA molecules and SO_4^{2-} ions adsorbed on the copper surface respectively.

The certain addition of KI to the PA SAMs in H_2SO_4 solution can significantly reduce the corrosion rate of copper due to the higher adsorption ability of I^-, which enhances the adsorption of the positively charged inhibitor molecules and reduces the dissolution of copper.

$$Cu + I^- \leftrightarrow CuI^-_{ads} \quad (11)$$

$$CuI^-_{ads} + PAH^+ \leftrightarrow CuI^-_{ads}PAH^+_{ads} \quad (12)$$

The Table 8 shows that both the inhibition abilities of PA alone and PA with I^- are quite in a good position.

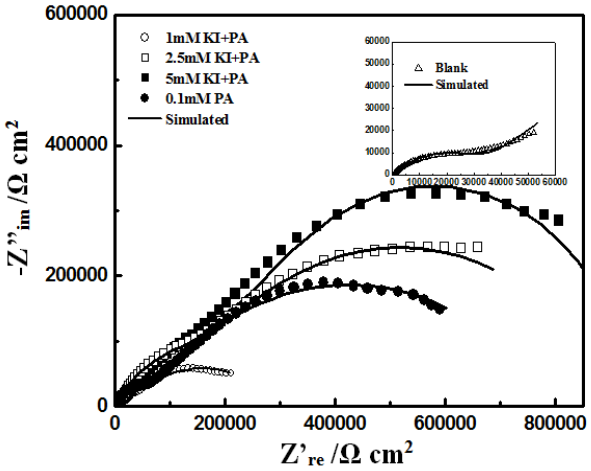

Figure 7. EIS plots of copper in 0.5 M H_2SO_4 solution in the absence and presence of PA SAMs formed in 0.1 mM PA solution in combination with different concentrations of KI.

Table 7. Synergistic parameters (S_1) for the different concentration of KI from EIS and potentiodynamic polarization methods.

KI concentration（mM）	Synergism parameter (S_1)	
	EIS method	Polarization method
1	0.766	0.997
2.5	2.70	2.45
5	3.72	3.77

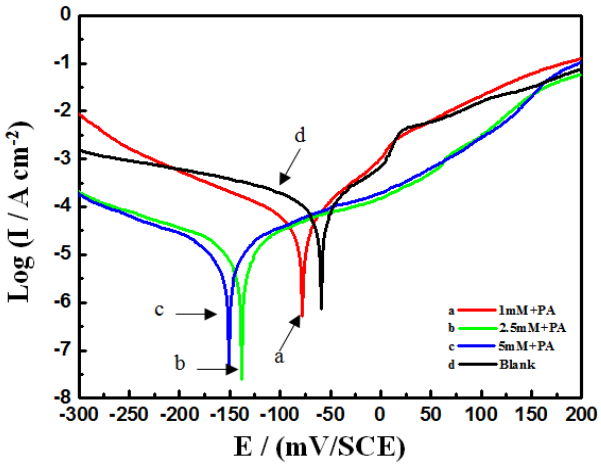

Figure 8. Potentiodynamic polarization curves for copper in 0.5 M H_2SO_4 solution in the absence and presence of PA SAMs formed in 0.1 mM PA solution in combination with different concentrations of KI.

Table 8 Compare of different inhibition efficiency (η) in different references.

Inhibitor	η %		Mixed with I^- (η %)	Reference number
	EIS	Potentiodynamic polarization		
Phytic Acid (This work)	84.5	83.3	90	
Phytic Acid	82.2	87.4		12
Cysteamine	69.2	77.9		1
Phytic Acid	82.6	90.6		17
Rrhodanine	98.8		99.9	47
1-[(1',2'-dicarboxy)ethyl]-benzotriazol	63	62	85	60

4. Conclusions

(1) The addition of PA SAMs on the copper surface in 0.5 M H_2SO_4 solution shows limited inhibition properties.
(2) PA molecules act as a kind of mixed type inhibitor adsorbed at the surface via P-O and the cyclohexyl ring.
(3) Adsorption of PA SAMs on copper surface obeys the Langmuir isotherm and is a chemical fashion.
(4) There is synergistic effect from PA SAMs and I^- due to the addition of I^- enhancing the inhibition efficiency significantly.

Acknowledgements

This work is supported by the National Natural Science Foundation of China (Grant No. 21073121), and PCSIRT (IRT1269).

Notes and References

The Education Ministry Key Lab of Resource Chemistry, Shanghai Key Laboratory of Rare Earth Functional Materials and Department of Chemistry, Shanghai Normal University, Shanghai, 200234, P. R. China.
*Corresponding authors: Fax: +86 021 64322511. haifengyang@yahoo.com (Hai-Feng Yang)

†Electronic Supplementary Information (ESI) available: [details of any supplementary information available should be included here]. See DOI: 10.1039/b000000x/

1 P. Song, X.-Y. Guo, Y.-C. Pan, S. Shen, Y.q. Sun, Y. Wen and H.-F. Yang, Insight in cysteamine adsorption behaviors on the copper surface by electrochemistry and Raman spectroscopy, Electrochim. Acta **89** (2013) 503-509.
2 E.-S.M. Sherif, Effects of 2-amino-5-(ethylthio)-1, 3, 4-thiadiazole on Copper Corrosion As a Corrosion Inhibitor in 3% NaCl Solutions, Appl. Surf. Sci. **252** (2006) 8615-8623.
3 K.F. Khaled, Guanidine Derivative As a New Corrosion Inhibitor for Copper in 3% NaCl Solution, Mater. Chem. Phys. **112** (2008) 104-111.
4 T.T. Qin, J. Li, H.Q. Luo, M. Li and N.B. Li, Corrosion Inhibition of Copper by 2, 5-dimercapto-1, 3, 4-thiadiazole Monolayer in Acidic Solution, Corros. Sci. **53** (2011) 1072-1078.
5 A.H. Jafari, S.M.A. Hosseini and E. Jamalizadeh, Investigation of Smart Nanocapsules Containing Inhibitors for Corrosion Protection of Copper, Electrochim. Acta **55** (2010) 9004-9009.
6 P. C. Okafor and Y.G. Zheng, Synergistic Inhibition Behaviour of Methylbenzyl Quaternary Imidazoline Derivative and Iodide Ions on Mild Steel in H_2SO_4 Solutions, Corros. Sci. **51** (2009) 850-859.
7 Y.-C. Pan, Y.Wen, X.-Y. Guo, P.Song, S.Shen, Y.-P. Du and H.-F. Yang, 2-Amino-5-(4-pyridinyl)-1,3,4-thiadiazole monolayers on copper surface: Observation of the relationship between its corrosion inhibition and adsorption structure, Corros. Sci. **73** (2013) 274-280.
8 Y.-C. Pan, Y. Wen, L.-Y. Xue, X.-Y. Guo and H.-F. Yang, Adsorption Behavior of Methimazole Monolayers on a Copper Surface and Its Corrosion Inhibition, J. Phys. Chem. C **116** (2012) 3532-3538.
9 Y. Feng, K.S. Siow, W.K. Teo and A.K. Hsieh, The Synergistic Effects of Propargyl Alcohol and Potassium Iodide on the Inhibition of Mild Steel in 0.5 M Sulfuric Acid Solution, Corros. Sci. **41** (1999) 829-852
10 H.L. Wang, R.B. Liu and J. Xin, Inhibiting Effects of Some Mercapto-triazole Derivatives on the Corrosion of Mild Steel in 1.0 M HCl Medium, Corros. Sci. **46** (2004) 2455-2466.
11 G. Mu, X. Li, Inhibition of Cold Rolled Steel Corrosion by Tween-20 in Sulfuric Acid: Weight Loss, Electrochemical and AFM Approaches, J. Coll. Interf. Sci. **289** (2005) 184-192.
12 S. Shen, X.Y. Guo, P. Song, Y.C. Pan, H.Q. Wang, Y. Wen and H.-F. Yang, Phytic acid adsorption on the copper surface: Observation of electrochemistry and Raman spectroscopy, Appl. Surf. Sci. **276** (2013) 167-173.
13 Y.H. Wang and J.B. He, Corrosion Inhibition of Copper by Sodium Phytate in NaOH Solution: Cyclic Voltabsorptometry for *in Situ* Monitoring of Soluble Corrosion Products, Electrochim. Acta **66** (2012) 45-51.
14 H.F. Yang, Y. Yang, H. Liu, Z.R. Zhang, G.L. Shen and R.Q. Yu, Formation of Inositol Hexaphosphate Monolayers at the Copper Surface from a Na-salt of Phytic Acid Solution Studied by in Situ Surface

Enhanced Raman Scattering Spectroscopy, Raman Mapping and Polarization Measurement, Anal. Chim. Acta **458** (2005) 159-165.

15 H.F. Yang, J. Feng, Y.L. Liu, Y. Yang, Z.R. Zhang, G.L. Shen and R.Q. Yu, Electrochemical and Surface Enhanced Raman Scattering Spectroelectrochemical Study of Phytic Acid on the Silver Electrode, J. Phys. Chem. B **108** (2004) 17412-17417.

16 R. Zhang, H.F. Yang, Y. P. Sun, W. Song, X. Zhu, N. Wang, Y. Wang, Y.C. Pan and Z.R. Zhang, Competitive Adsorption of 4-Methyl-4*H*-1,2,4-triazole-3-thiol and Na Salt of Phytic Acid on a Silver Surface: Raman Spectral and Electrochemical Observations, J. Phys. Chem. C **113** (2009) 9748-9754.

17 C. Hao, R.H. Yin, Z.Y. Wan, Q.J. Xu and G.D. Zhou, Electrochemical and Photoelectrochemical Study of the Self-Assembled Monolayer Phytic Acid on Cupronickel B30, Corros. Sci. **50** (2008) 3527-3533.

18 Y. Shinohara, Y. Ota, H. Yamamoto and H. Kunieda, Japanese Patent, Japanese Kokai Tokkyo Koho JP 1986 61 030,685 [86 30 685].

19 A.-R. El-Sayed, U. Harm, K.-M. Mangold and W. Fürbeth, Protection of Galvanized Steel from Corrosion in NaCl Solution by Coverage With Phytic Acid SAM Modified with Some Cations and Thiols, Corros. Sci. **55** (2012) 339-350.

20 S.S. Abdel Rehim, O.A. Hazzazi, M.A. Amin and K.F. Khaled, On the Corrosion Inhibition of Low Carbon Steel in Concentrated Sulphuric Acid Solutions. Part I: Chemical and Electrochemical (AC and DC) Studies, Corros. Sci. **50** (2008) 2258-2271.

21 S.A. Umoren, E.E. Ebenso, P.C. Okafor, U.J. Ekpe and O. Ogbobe, Effect of Halide Ions on the Corrosion Inhibition of Aluminium in Alkaline Medium Using Polyvinyl Alcohol, J. Appl. Poly. Sci. **103** (2006) 2810-2816

22 H. Tavakoli, T. Shahrabi and M.G. Hosseini, Synergistic Effect on Corrosion Inhibition of Copper by Sodium Dodecylbenzenesulphonate (SDBS) and 2-mercaptobenzoxazole, Mater. Chem. Phys. **109** (2008) 281-286.

23 P.C. Okafor, E.E. Oguzie, G.E. Iniama, M.E. Ikpi and U.J. Ekpe, Corrosion Inhibition Properties of Thiosemicarbazone and Semicarbazone Derivatives in Concentrated Acid Environment, Glob. J. Pure Appl. Sci. **14** (2008) 89-95.

24 C. Jeyaprabha, S. Sathiyanarayanan and G. Venkatachari, Influence of Halide Ions on The Adsorption of Diphenylamine on Iron in 0.5 M H_2SO_4 Solutions, Electrochim. Acta **51** (2006) 4080-4088.

25 J.C. Love, L.A. Estroff, J.K. Kriebel, R.G. Nuzzo and G.M. Whitesides, Self-Assembled Monolayers of Thiolates on Metals as a Form of Nanotechnology, Chem. Rev. **105** (2005) 1103-1169.

26 A. Ulman, Formation and Structure of Self-Assembled Monolayers, Chem. Rev. **96** (1996) 1533-1554.

27 T. Shimura and K. Aramaki, Protection of Iron Against Corrosion by Coverage with Ultrathin Two-dimensional Polymer Films of a Hydroxymethylbenzene Self-Assembled Monolayer Aanchored by the Formation of a Covalent Bond, Corros. Sci. **50** (2008) 292-300.

28 M.L. Lewis, L. Lendung and K.T. Carron, Surface Structure Determination of Thin Films of Benzimidazole on Copper Using Surface Enhanced Raman Spectroscopy, Langmuir **9** (1993) 186-191.

29 M.M. Musiani, G. Mengoli, M. Fleischmann and R.B. Lowry, An Electrochemical and SERS Investigation of the Influence of pH on the Effectiveness of Some Corrosion Inhibitors of Copper, J. Electroanal. Chem. **217** (1987) 187-202.

30 J.L. Yao, B. Ren, Z.F. Huang, P.G. Cao, R.A. Gu and Z.Q. Tian, Extending Surface Raman Spectroscopy to Transition Metals for Practical Applications IV. A Study on Corrosion Inhibition of Benzotriazole on Bare Fe Electrodes, Electrochim. Acta **48** (2003) 1263-1271.

31 G.M. Brown and G.A. Hope, In-situ Spectroscopic Evidence for the Adsorption of SO^{2-}_4 Ions at a Copper Electrode in Sulfuric Acid Solution, J. Electroanal. Chem. **382** (1995) 179-182.

32 X.M. Wang, H.Y. Yang and F.H. Wang, An Investigation of Benzimidazole Derivative as Corrosion Inhibitor for Mild Steel in Different Concentration HCl Solutions, Corros. Sci. **53** (2011) 113-121.

33 X.M. Wang, H.Y. Yang and F.H. Wang, A Cationic Gemini-surfactant as Effective Inhibitor for Mild Steel in HCl Solutions, Corros. Sci. **52** (2010) 1268-1276.

34 X.M. Wang, H.Y. Yang and F.H. Wang, Inhibition Performance of a gemini Surfactant and Its Co-adsorption Effect with Halides on Mild Steel in 0.25 M H_2SO_4 Solution, Corros. Sci. **55** (2012) 145-152.

35 M.K. Pavithra, T.V. Venkatesha, K. Vathsala and K.O. Nayana, Synergistic Effect of Halide Ions on Improving Corrosion Inhibition Behaviour of Benzisothiozole-3-piperizine Hydrochloride on Mild Steel in 0.5 M H_2SO_4 Medium, Corros. Sci. **52** (2010) 3811-3819.

36 S.L. Li, H.Y. Ma, S.B. Lei, R. Yu, S.H. Chen and D.X. Liu, Inhibition of Copper Corrosion With Schiff Base Derived from 3-methoxysalicylaldehyde and o-phenyldiamine in Chloride Media, Corrosion **54** (1998) 947-954.

37 E.A. Noor, Evaluation of Inhibitive Action of Some Quaternary N-heterocyclic Compounds on the Corrosion of Al-Cu Alloy in Hydrochloric Acid, Mater. Chem. Phys. **114** (2009) 533-541.

38 E. McCafferty, Validation of corrosion rates measured by the Tafel extrapolation method, Corros. Sci. 47 (2005) 3202-3215.

39 W. Li, Q. He, S. Zhang, C. Pei and B. Hou, Some New Triazole Derivatives as Inhibitors for Mild Steel Corrosion in Acidic Medium, J. Appl. Electrochem. **38** (2008) 289-295.

40 F. Bentiss, M. Traisnel, N. Chaibi, B. Mernari, H. Vezin and M. Lagrenee, 2,5- bis(n-methoxyphenyl)-1,3,4-oxadiazoles Used as Corrosion Inhibitors in Acidic Media: Correlation Between Inhibition Efficiency and Chemical Structure, Corros. Sci. **44** (2002) 2271-2289.

41 N. Fe´lidj, J. Aubard, G. Le´vi, J.R. Krenn, M. Salerno, G. Schider and B. Lamprecht, A. Leitner, F.R. Aussenegg, Controlling the Optical Response of Regular Arrays of Gold Particles for Surface-Enhanced Raman Scattering, Phys. ReV. B **65** (2002) 075419 (9 pages).

42 A.D. McFarland, M.A.Young, J.A. Dieringer and R.V. Duyne Wavelength-Scanned Surface-Enhanced Raman Excitation Spectroscopy, J. Phys. Chem. B **109** (2005) 11279-11285.

43 M. Moskovits, Surface selection rules, J. Chem. Phys. **77** (1982) 4408 (9 pages).

44 M. Moskovits and J.S. Suh, Surface Selection Rules for Surface-Enhanced Raman Spectroscopy: Calculations and Application to the Surface-Enhanced Raman Spectrum of Phthalazine on Silver, J. Phys. Chem. **88** (1984) 5526-5530.

45 Yu.P. Khodyrev, E.S. Batyeva, E.K. Badeeva, E.V. Platova, L. Tiwari and O.G. Sinyashin, The Inhibition Action of Ammonium Salts of O,O′-dialkyldithiophosphoric Acid on Carbon Dioxide Corrosion of Mild Steel, Corros. Sci. **53** (2011) 976-983.

46 S.A. Umoren ,Y.Li and F.H. Wang, Electrochemical Study of Corrosion Inhibition and Adsorption Behaviour for Pure Iron by Polyacrylamide in

H_2SO_4: Synergistic Effect of Iodide Ions, Corros. Sci. **52** (2010) 1777-1786.

47 R. Solmaz, E. A. Şahin, A. Dönerb and G. Kardaş, The Investigation of Synergistic Inhibition Effect of Rrhodanine and Iodide Ion on The Corrosion of Copper in Sulphuric Acid Solution, Corros. Sci. **53** (2011) 3231-3240.

48 X. Zhou, H.Y. Yang and F.H. Wang, [BMIM]BF4 Ionic Liquids as Effective Inhibitor for Carbon Steel in Alkaline Chloride Solution, Electrochim. Acta **56** (2011) 4268-4275.

49 M.S. Morad, Corrosion Inhibition of Mild Steel in Sulfamic Acid Solution by S-Containing Amino Acids, J. Appl. Electrochem. **38** (2008) 1509-1518.

50 G. Avci, Inhibitor effect of N,N-methylenediacrylamide on Corrosion Behavior of Mild Steel in 0.5M HCl, Mater. Chem. Phys. **112** (2008) 234-238..

51 L.J. Li, X.P. Zhang, J.L. Lei, J.X. He, S.T. Zhang and F.S. Pan, Adsorption and Corrosion Inhibition of Osmanthus Fragran Leaves Extract on Carbon Steel, Corros. Sci. **63** (2012) 82-90.

52 X.H. Li, S. Deng and H. Fu, Inhibition Effect of Methyl Violet on the Corrosion of Cold Rolled Steel in 1.0 M HCl Solution, Corros. Sci. **52** (2010) 3413-3420.

53 O.K. Abiola and N.C. Oforka, Adsorption of (4-amino-methyl-5-pyrimidinyl methylthio) acetic acid on mild steel from hydrochloric acid solution (HCl)-Part 1, Mater. Chem. Phys. **83** (2004) 315-322.

54 S.A. Umoren, Y. Li and F.H. Wang, Synergistic Effect of Iodide Ion and Polyacrylic Acid on Corrosion Inhibition of Iron in H_2SO_4 Investigated by Electrochemical Techniques, Corros. Sci. **52** (2010) 2422-2429.

55 E.E. Oguzie, G.N. Onuoha and A.I. Onuchukwu, Inhibitory Mechanism of Mild Steel Corrosion in 2 M Sulphuric Acid Solution by Methylene Blue Dye, Mater. Chem. Phys. **89** (2005) 305-311..

56 S.A. Umoren, O. Ogbobe, I.O. Igwe and E.E. Ebenso, Inhibition of Mild Steel Corrosion in Acidic Medium Using Synthetic and Naturally Occurring Polymers and Synergistic Halide Additives, Corros. Sci. **50** (2008) 1998-2006.

57 S.S. Abdel Rehim, O.A. Hazzazi, M.A. Amin and K.F. Khaled, On the Corrosion Inhibition of Low Carbon Steel in Concentrated Sulphuric Acid Solutions. Part I: Chemical and Electrochemical (AC and DC) Studies, Corros. Sci. **50** (2008) 2258-2271.

58 X. Li, S. Deng, H. Fu and G. Mu, Synergism Between Rare Earth Cerium(IV) Ion and Vanillin on the Corrosion of Cold Rolled Steel in 1.0 M HCl Solution, Corros. Sci. **50** (2008) 3599-3609.

59 D.Q. Zhang, L.X. Gao and G.D. Zhou, Synergistic Effect of 2-mercaptobenzimidazole and KI on Copper Corrosion Inhibition in Aerated Sulfuric Acid Solution, J. Appl. Electrochem. **33** (2003) 361-366.

60 D. Q. Zhang, X.-M. He, Q.-R. Cai, L.-X Gao and G.S. Kim, Arginine Self-assembled Monolayers Against Copper Corrosion and Synergistic Effect of Iodide Ion, J. Appl. Electrochem. **39** (2009) 1193-1198.

61 D.P. Schweinsberg, S.E. Bottle and V. Otieno-Alego, Electrochemical Study of the Synergistic Effect of 1-[(1',2'-dicarboxy)ethyl]-benzotriazol and KI on the Dissolution of Copper in Aerated Sulfuric Acid, J. Appl. Electrochem. **27** (1997) 161-168

62 M.A. Amin and K.F. Khaled, Copper Corrosion Inhibition in O_2-saturated H_2SO_4 Solutions, Corros. Sci. **52** (2010) 1194-1204.

63 R. Solmaz, G. Kardaş, M. Çulha, B. Yazıcı and M. Erbil, Investigation of Adsorption and Inhibitive Effect of 2-mercaptothiazoline on Corrosion of Mild Steel in Hydrochloric Acid Media, Electrochim. Acta **53** (2008) 5941-5952.

Graphical Abstract

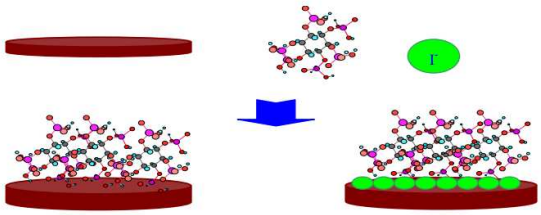

Electrochemical and Raman observations show synergistic inhibition of phytic acid and I^- for copper from corrosion in acid solution.